Matching of EDM Prototype Ring Circumference to Injection Ring Circumference

R. Talman and J. Talman

January 1, 2020

Abstract

Pursuant to CERN Yellow Report (CYR) "Storage Ring to Search for Electric Dipole Moments of Charged Particles: Feasibility Study" this report expands upon Chapter 7 "The EDM Prototype Ring (PTR)", with special emphasis on optimizing the PTR circumference for the injection line beam polarization preserving filling process. For concreteness in this report, the COSY ring (with $\mathcal{C}_{\mathrm{INJ}} = 182\,\mathrm{m}$ circumference) is taken as the injection ring prototype, but the methodology can be easily adapted to other circumference choices. The main issue, to permit single bunch train transfer, is that INJ and PTR ring circumferences should be related by "easy" rational fractions–here, for INJ/PTR we consider only the fractions 1/2, 3/4, and 1/1. Other significant issues are availability of free straight section length for needed apparatus, required electric field maximum, and overall PTR cost.

1 All-electric ring scaling from the CERN Yellow Report

1.1 Initial assumptions

There has been concern whether or not the PTR ring described in the CERN Yellow Report (CYR)[1] has sufficient total free drift space for required diagnostic and beam handling equipment. One approach could be to migrate from rounded-square ring shape to racetrack-shape, to make more space available. I have come to believe that this is a bad idea for two reasons.

Injection at a corner, as shown in Figure 1, seems economical and ideally symmetric for injecting counter-circulating beams. This symmetry would be lost in a race-track configuration, complicating the task of exactly matchingh beam profiles. A probably more serious problem is that the focusing implied by long straight sections precludes the possibility of tuning the vertical tune Q_y down close to zero. This sacrifices self-magnetometry sensitivity, which scales as $1/Q_y$.

In this report I therefore consider only rounded-square lattice shapes. It is convenient that the required ring scaling was already faced in the far greater range from PTR scale to Holy-Grail scale. I also assume the quadrupoles labeled "D" in Figure 1, and differently in Figure 2, located at the mid points of long straight sections, will not be needed.

Only three lattices are considered: one with the same circumference as COSY, one with half-COSY circumference (roughly the same as the CYR-nominal PTR ring) and one half way between these two cases. With COSY taken as the choice for INJ, the ideal PTR circumferences are $\mathcal{C}_{\mathrm{PTR}} = 91\,m, 136.5\,m, and 182\,\mathrm{m}$; (with designated file-names identifications "-0p5-COSY", "-0p75-COSY", and "-1p0-COSY).

Furthermore I have chosen to emphasize the (difficult) low Q_y (high β_y) region. (As demonstrated in Chapter 7 of the CYR) the quite numerous QF and QD quadrupoles provide ample tuning range for both
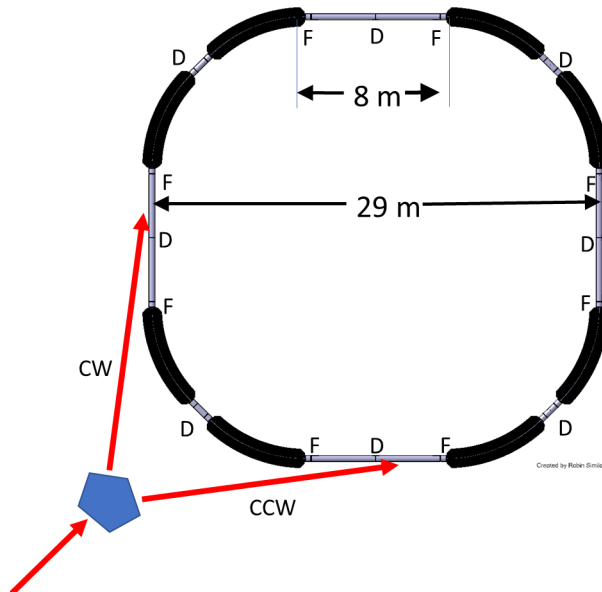
Figure 1: (Copied from CYR) the basic layout of the prototype ring consists of 8 dual, superimposed electric and magnetic bends; 2 families of quadrupoles—focusing (F) and de-focusing (D); with an optional skew quadrupole family at mid-points of the four 8 m long straight sections. The total circumference, as described in the CYR, was about 100 m. The three lattices described in the present report have nominal circumferences of 90.8 m, 136.5 m, and 183 m, intentionally (but only approximately, so far) adjusted close to 1/2, 2/3, and 1/1 times the COSY ring circumference. Otherwise the ring designs are unchanged from the CYR.

tunes, Q_x and Q_y. The three rings in this report remain (at least nominally) capable of being tuned down arbitrarily close to the $Q_x = Q_y = 0$) limit. This capability is provided by altering gradient, very-weakly focusing $m \neq 0$ electrode shaping. But, for most ring commissioning, the focusing provided by QF and QD quads will be dominant, making the electrode shapes, effectively, purely cylindrical (i.e. $m \approx \pm 0$).

Focusing on the technically-difficult, low Q_y, limit makes the cases addressed in this report hypersensitive. Strengthening the QF/QD focusing from this limit can be performed easily. More technical discussion of these points has already been given in CYR Chapter 7.

All parameter determinations in this report are based on coordinating two entirely different ring design programs. One of these, referred to as "MAPLE", is based on Wollnik linear transfer matrices, and is essentially equivalent to Valeri Lebedev's similar program[2]—traditionally there has been quite good agreement between Valeri's and my versions of these explicitly linearized Courant-Snyder codes.

The other ring design program is referred to as "ETEAPOT"[3][4]. Patterned after TEAPOT[5][6][7], developed for the SSC by Lindsay Schachinger and me, ETEAPOT is based entirely on particle tracking. In this approach, ring transfer matrices are calculated as outputs rather than being provided analytically as inputs. Traditional lattice parameters, such as tunes, Twiss functions, and dispersions, are obtained from the derived transfer maps (including higher than linear order, if necessary).

The figures in this report show that agreement between MAPLE and ETEAPOT models, though excellent, is not perfect. I think the small discrepancy is due to an approximation built into ETEAPOT (which is nominally exact for $m = 1$ electrode shapes, but needs to be exrapolated to the $m = \pm 0.002$ (almost exactly "cylindrical") design electrode shapes. This extrapolation range is large enough for its linearity assumption to be questionable.

This discrepancy remains to be investigated. For now a single parameter, the same for all three rings, constrains the maximum vertical beta function values obtained by MAPLE and ETEAPOT to agree. (Compare Figures 5 and 6, and accompanying tables, 3, 4, and 5, where the free parameter is indicated a an argument of ETEAPOT[-0.032].) As a result the vertical beta functions obtained by ETEAPOT

differ by as much as ten percent from those calculated by MAPLE (in the hypersensitive high β_y region). This level of disagreement seems ignorable for the time being. As already mentioned, this comparison has been made in the "fine-tuning limit" for which the vertical tune is close to zero.

1.2 Adjusting PTR design based on CYR "Holy Grail" scaling prescription

This section describes a four parameter lattice design for a complete family of stable all-electric storage rings, ranging from the PTR ring at the small radius, low energy end, to a full scale, large radius, high energy end. This is the same prescription, as described in the CYR report, for scaling down from the "Holy Grail" design to the nominal PTR design. This skeletal PTR prototype lattice design, copied from CYR, is shown in Figure 2. In all considered ring designs, for flexibility, focusing is provided both
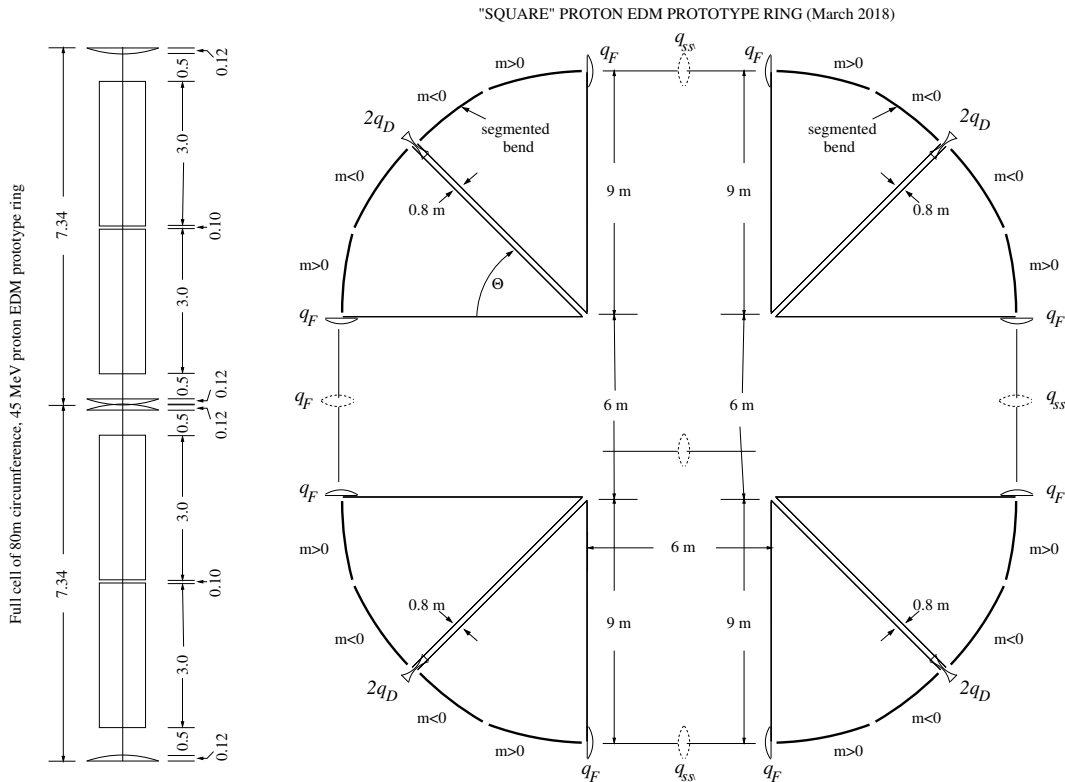

Figure 2: Lattice layouts for proposed lattice half-cell (left) and full ring (right). The accumulated drift length is not enough for the ring to operate "below transition". When scaling up to the eventual, full energy, all-electric ring, from four-fold to sixteen-fold symmetry, with drift lengths and bend lengths preserved (but bend angles four times less) the total circumference is to be about 500 m and operation will be well below transition.

by separated-function electric quadrupoles, and by (very weak) alternating-gradient, combined-function, electrode-shape focusing. The designs in this report assume extremely weak electrode-shape focusing but with predominently lumped quadrupole focusing for routine operations.

The scaling in the present report uses the scaling prescription explained in the CYR, which introduced a four-parameter family of all-electric rings. The four parameters for the rings in that report are exhibited in the upper table of Table 1. A corresponding table for the present report is exhibited in the ower table of Table 1. By introducing the ratio $\rho_{\text{L/R}}$=L_LONG_STRAIGHT/R_NOMINAL$\approx$ 0.6, also shown in the lower table, it can be seen that, over the smaller range of bending radii considered in this report, the

number of free parameters needed is (roughly) reduced from four to three. (For variation over the full

Table 1: (Copied from CYR) the four major parameters for scaling between full scale ring and prototype ring. They describe a continuum of stable, all-electric storage rings ranging from small, low energy to large, high energy. Their uppercase names make these parameters easily recognizable in lattice description files. The remaining (minor) parameters are given in Table 2.

The upper table (copied fro CYR) gives parameters approptiate for variable proton energy. The lower table (specific to this report) gives parameters for variable PTR circumference.

parameter	E_30MeV	EM_35MeV	EM_45MeV	EM_55MeV	E_233MeV
R_NOMINAL [m]	9.0	9.0	9.0	9.0	40.0
L_LONG_STRAIGHT [m]	6.0	6.0	6.0	6.0	14.8
N_SUPER	4	4	4	4	16
M_NOMINAL	0.1	0.1	0.1	0.1	0.1

parameter	E-PTR2-0p5-COSY	E-PTR2-0p75-COSY	E-PTR2-1p0-COSY
R_NOMINAL [m]	10.0	15.4	21.0
L_LONG_STRAIGHT [m]	6.00=0.60 x R_NOMINAL	8.932=0.58 x R_NOMINAL	11.76=0.56 x R_NOMINAL
N_SUPER	4	4	4
M_NOMINAL	±0.002	±0.002	±0.002

PTR to "Holy Grail" range, the adopted scaling relations follow: the field index scales inversely with super-periodicity N_SUPER; with $m = \pm$M_NOMINAL being the field indices of the prototype ring, the scaling relation is $m = \pm$M_NOMINAL*4/N_SUPER. Lattice names are in the column headings. Minor (unchanged) parameter valus are indicated in Table 2, which has also been copied, unchanged, from the CYR.

Table 2: (Copied from CYR, and unchanged for this report,) minor geometric parameters: Theta, $r0$, leh, $lss = 0.8$ m, and $llsh$ are, respectively, bend/half-period, bend radius, bend-half-length, short-straight-length, and long-straight-half-length. $K0$ is proton kinetic energy and $\pm m_{in}$ are alternating field index values. Minor kinetic parameters: lq is quad length, qF and qD are quad strengths, $gBy2$ is half-gap width, Q_x and Q_y are tunes.

lattice name	K0 [MeV]	m_in	Theta [r]	r0 [m]	leh [m]	llsh [m]	lq [m]	qF/qD [1/m]	circ. [m]	gBy2 [m]	Q_x/Q_y
E_30MeV	0.0300	0.100	0.785	9	3.53	2.60	0.2000	∓0.01	83.7	0.035	1.768/0.093
EM_45MeV	0.0450	0.100	0.785	9	3.53	2.60	0.2000	∓0.01	83.7	0.035	1.750/0.093
E_233MeV	0.2328	0.025	0.196	40	3.93	7.00	0.2000	∓0.0025	501	0.015	1.815/0.145

(For what seems like the most promising "three-quarters COSY" case) detailed lattice descriptions (needed for computer processing) are contained in the following files (which supercede the corresponding files referenced in CYR, are are also available on request). Since the first two of these files are quite short (yet provide a complete idealized lattice description and are easily humanly-decipherable) they are attached as appendices to this report. The remaining two files, produced by XSLT software, merge the first two files into long, computer readable files that need to be readable by human beings only for debugging purposes.

E-PTR2-0p75-COSY-con_xml: ".xml" file containing all parameters (both symbols and their values) for a small proton EDM prototype ring, including (symbolic) parameters for scaling to the large (500 m circumference) all-electric proton EDM ring.

E-PTR2-0p75-COSY-nocon_xml: Symbolic ".xml" file describing the idealized lattice design. (Actually this file does not depend on ring radius–it is therefore identical to E-PTR2-0p5-COSY-nocon_xml and E-PTR2-1p0-COSY-nocon_xml).

E-PTR2-0p75-COSY.adxf: Numerical ".adxf" file describing idealized lattice design.

E-PTR2-0p75-COSY.sxf: Numerical ".sxf" file describing fully-instantiated lattice design (though without differentiated (i.e. individualized) parameter values.)

Initially, for both prototype and full-scale ring, the horizontal tune was expected to be just below 2.0 and the vertical tune much less than 1.0, and tuneable to a value as low as 0.02. The ultra-low vertical tune requirement is needed to reduce the vertical restoring force, therby enhancing the beam "self-magnetometry" sensitivity to beam displacement caused by radial magnetic field.

(As an aside, it can now be mentioned, that the doubly-magic EDM measurement method possibility avoids the need for ultraweak vertical focusing, allowing the focusing to be much stronger than was initially anticipated. A very thorough and valuable 2015 study by V. Lebedev[2] analysed two frozen-spin all-electric designs, one very weak-focusing, the other stronger focusing. With ultra-low vertical tune no longer necessary, the scaled down PTR can be said to more nearly correspond to the stronger-focusing ring Valeri favoured.)

For the full-scale ring the correspondingly smaller tune advance per super-period causes the focusing to be weaker. This is what permits the long straight sections of the full scale ring to be almost doubled, compared to the prototype (from $6\,\mathrm{m}$ to $14.8\,\mathrm{m}$). This has the beneficial (perhaps even obligatory) effect, for the full-scale ring, of operating "below transition". This ameliorates intrabeam scattering, as can be explained in connection with stochastic cooling. (Conversely, this is one respect in which the prototype ring optics still is a not-quite-faithful prototype.) This choice was made to reduce the prototype size.

2 Determination of Twiss Functions From Transfer Matrices

Like the magnetic accelerator simulation code TEAPOT, the electric accelerator code ETEAPOT, does not base particle tracking on theoretically-derived transfer matrices. Rather, a standard set of small amplitude particles are tracked (i.e. to satisfy Newton's force law). Then, by differencing the outputs, transfer matrices are extracted—in what amounts to numerical differentiation. Then, from the transfer matrices, the lattice twiss functions are derived. Because this is an unconventional approach, the following sections explain the approach in more detail.

2.1 Analysis of the Once-Around Transfer Matrix at the Origin

In this section x and y and ct subscripts will be suppressed, and only transverse evolution is to be discussed. The most general transfer matrix is a six-by-six matrix $\mathbf{M}(s_i, s_j)$, which propagates a phase space vector $\mathbf{x}(s_i)$ at s_i, to its value $\mathbf{x}(s_j)$ at s_j;

$$\mathbf{x}(s_j) = \mathbf{M}(s_i, s_j)\,\mathbf{x}(s_i). \tag{1}$$

ETEAPOT starts by assigning coordinates at the origin, $s_0 = 0$, to the particles in a standard bunch (as described earlier), and then evolves the standard bunch and records the coordinates $\mathbf{x}(s_i)$ at all points s_i. From these results the transfer matrices $\mathbf{M}(0, s_i)$ can be calculated (also as described earlier). By definition

$$\mathbf{M}(0,0) = \mathbf{I}, \tag{2}$$

where $\mathbf{I}$ is the 6×6 identity matrix.

To extract Twiss lattice functions one needs periodic, "once-around" transfer matrices, distinguished by overhead tildes, and defined by

$$\widetilde{\mathbf{M}}(s_i) \equiv \mathbf{M}(s_i, s_i + \mathcal{C}_0) = \mathbf{M}(0, s_i)\,\mathbf{M}(s_i, \mathcal{C}_0). \tag{3}$$

where $\mathcal{C}_0$ is the circumference of the design orbit; the final step has been taken because knowledge of $s_i + \mathcal{C}_0$ requires tracking for more than one complete turn, but we are assuming that tracking has been done only for exactly one complete turn. Propagation from $s = \mathcal{C}_0$ to $\mathcal{C}_0 + s_i$ is the same as propagation from $s = 0$ to s_i. The Twiss parameterization of (one partitioned diagonal 2×2 block of) such a once-around, symplectic transfer matrix is

$$\widetilde{\mathbf{M}}(s_i) = \begin{pmatrix} \cos\mu + \alpha\sin\mu & \beta\sin\mu \\ -\frac{1+\alpha^2}{\beta}\sin\mu & \cos\mu - \alpha\sin\mu \end{pmatrix}. \tag{4}$$

Extraction of the α_0 and β_0, the Twiss parameters at the origin, can start from

$$\cos\mu = \frac{1}{2}\left(\widetilde{\mathbf{M}}_{11}(0) + \widetilde{\mathbf{M}}_{22}(0)\right), \tag{5}$$

which fixes $\cos\mu$. Because of sign ambiguity, this determines only $|\sin\mu|$. One also has the relations

$$\beta_0 = \left|\frac{\widetilde{\mathbf{M}}_{12}(0)}{\sin\mu}\right|. \tag{6}$$

and

$$\alpha_0 = \frac{1}{2\sin\mu}\left(\widetilde{\mathbf{M}}_{11}(0) - \widetilde{\mathbf{M}}_{22}(0)\right). \tag{7}$$

With β being positive by convention, from the 1,2 element, sign($\sin\mu$) can be seen to be the same as sign($\widetilde{\mathbf{M}}_{12}$). With $\cos\mu$ known, this fixes $\sin\mu$. Together, these relations fix $\sin\mu$, $\cos\mu$, α_0, and β_0.

Conventionally one also introduces a third Twiss parameter

$$\gamma_0 = \frac{1 + \alpha_0^2}{\beta_0}, \tag{8}$$

which can be obtained once β_0 and α_0 have been determined.

Because of the multiple-valued nature of inverse trig functions, these relations do not determine a unique value for μ. They do, however, determine the quadrant in phase space in which the angle μ resides. For sign($\sin\mu$)>0 the angle μ resides in the first or second quadrant, in which case the fractional tune is less than 1/2; otherwise the fractional tune is greater than 1/2. For sign($\cos\mu$)>0 the angle μ resides in the first or fourth quadrant, in which case the fractional tune is below 1/4 or above 3/4. These considerations fix the fractional parts of the tunes.

An "aliasing" or "integer-tune" ambiguity remains, however, which cannot, even in principle, be obtained from the once-around matrix. Only if both transverse tunes are less than 1 (which is hardly ever the case) would the tunes be equal to the fractional tunes that have been determined. In general, to obtain the integer tunes, it is necessary to analyse the turn by turn data at sufficiently closely-space intermediate points in the lattice.

2.2 Evolving the Twiss Functions Around the Ring

To find the Twiss parameters at an arbitrary location s_i in the ring requires the once-around transfer matrix $\widetilde{\mathbf{M}}(s_i)$. This can obtained most compactly by multiplying the equation

$$\mathbf{M}(0, s_j) = \mathbf{M}(s_i, s_j)\,\mathbf{M}(0, s_i) \tag{9}$$

on the right by $\mathbf{M}^{-1}(0, s_i)$ to produce

$$\mathbf{M}(s_i, s_j) = \mathbf{M}(0, s_j)\,\mathbf{M}^{-1}(0, s_i). \tag{10}$$

Substituting this with $s_j = \mathcal{C}_0$ into Eq. (3) produces

$$\widetilde{\mathbf{M}}(s_i) = \mathbf{M}(0, s_i)\,\widetilde{\mathbf{M}}(0)\,\mathbf{M}^{-1}(0, s_i). \tag{11}$$

Having obtained $\widetilde{\mathbf{M}}(s_i)$, the procedure described in the previous subsection can then be used to obtain $\alpha(s_i)$ and $\beta(s_i)$. But the integer tune ambiguity can, again, not be resolved. To resolve this ambiguity both x and y phases have to be tracked continuously through the lattice, requiring that they advance continuously and monotonically. (Later, at least in principle, the same ambiguity will have to be faced for longitudinal motion. But the integer longitudinal tune is almost always zero, so the problem is usually absent in the longitudinal case.)

ETEAPOT requires the lattice description to be in the form of an `.sxf` file. To be "legal" the granularity of such a file has to be fine enough that no phase can advance by more than a quarter integer

through any element in the file. Before working out the α and β function evolution, ETEAPOT first works out the total phase advances from the origin to every node specified by the `.sxf` file (or, if some elements are sliced more finely, by every node after slicing).

There is an alternative way of finding the betatron phase advances. It starts with a Twiss parameterization of $\mathbf{M}(0,s)$ from the origin to an arbitrary position s in the lattice;

$$\mathbf{M}(0,s) = \begin{pmatrix} \sqrt{\frac{\beta(s)}{\beta_0}}\Big(\cos\psi(s) + \alpha_0\sin\psi(s)\Big) & \sqrt{\beta_0\beta(s)}\,\sin\psi(s) \\ \cdot & \sqrt{\frac{\beta_0}{\beta(s)}}\Big(\cos\psi(s) - \alpha(s)\sin\psi(s)\Big) \end{pmatrix}. \tag{12}$$

The 2,1 element is quite complicated; it is not shown here since it will not be needed for the following analysis. Dividing the 1,1 element by the 1,2 element produces

$$\frac{\mathbf{M}_{1,1}(0,s)}{\mathbf{M}_{1,2}(0,s)} = \frac{\sqrt{\frac{\beta(s)}{\beta_0}}\Big(\cos\psi(s) + \alpha_0\sin\psi(s)\Big)}{\sqrt{\beta_0\beta(s)}\,\sin\psi(s)} = \frac{\cot\psi(s) + \alpha_0}{\beta_0}. \tag{13}$$

Rearranging this equation produces

$$\psi(s) = \tan^{-1}\frac{\mathbf{M}_{1,2}(0,s)}{\beta_0\mathbf{M}_{1,1}(0,s) - \alpha_0\mathbf{M}_{1,2}(0,s)}. \tag{14}$$

Like all inverse trigonometric formulas, this equation has multiple solutions. But, with the `.sxf` granularity being required to be fine enough, one can (in principle) sequentially obtain unique phases. With $\psi(s)$ starting from $\psi(0) = 0$, as s increases from s_i to s_{i+1} there is a unique solution of Eq. (14), $\psi(s_i) \geq \psi(s_{i-1})$ such that the function $\psi(s)$ increases monotonically, as required. Because the interval from $s_{i=1}$ to s_i is non-zero, ψ will, superficially, advance discontinuously; the correct solution is the least discontinuous. The same calculation has to be done for both the x and y betatron sectors. Unfortunately, even though, theoretically, the phase advances monotonically, numerical errors can cause Eq. (14) to give local phase decrease. This can cause Eq. (14) to give occasionally erratic results.

3 Tuning-up variable-circumference PTR properties

Figures 3 and 4 compare β_x evaluations for the three lattices studied for this report. Of the rings in this report, `E-PTR2-0p5` is the one closest to the prototype ring described in the CERN Yellow Report. The alternating gradient pole shape focusing, though ultraweak, by itself, barely produces vertical stability. "Geometric" focusing, though also not very strong, is capable of providing much stronger horizontal focusing, with horizontal tune Q_x greater than 1.0. For the following graphs, the QF and QD quads, arranged in FODO pattern, provide stronger focusing in both planes. As described in CYR, by strengthening QF and QD, there is a large tuning range over which Q_y can smoothly increase from barely above 0 to just below 1, and Q_x can smoothly decrease from barely below 2 to just above 1. The figure on the left is evaluated by ETEAPOT, the one on the right by linearized (Wollnik) formulas.

There is good qualitative agreement between MAPLE and ETEAPOT. Quantitative agreemen is not perfect though. This is at least partly due to a significantly large "perturbative" correction from the $m = 1$ electrode-shape focusing "Muñoz-Pavic" limit in which ETEAPOT is analtically exact, to the $m \approx 0$ "cylindrical" electrode case, aplicable in this, and all other rings in this report. Side-by-side horizontal beta function comparisons are exhibited in Figures 3 and 4. Vertical beta function comparisons are exhibited in Figures 5 and 6. Horizontal dispersion suctions are shown in Figure 7 and betatron tune accumuation plots are shown in Figure 8.

Along with other parameters, much the same lattice function information is shown in compressed tabular form in the tables shown right after the figures; Table 3, 4, and 5,
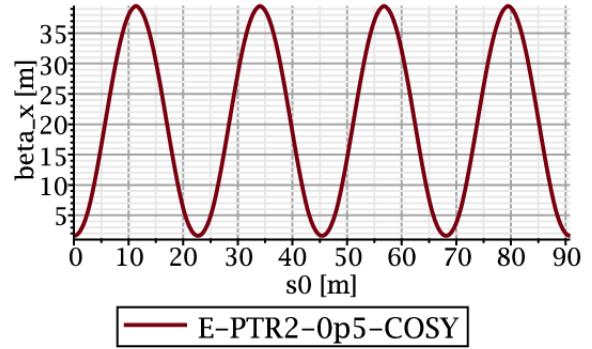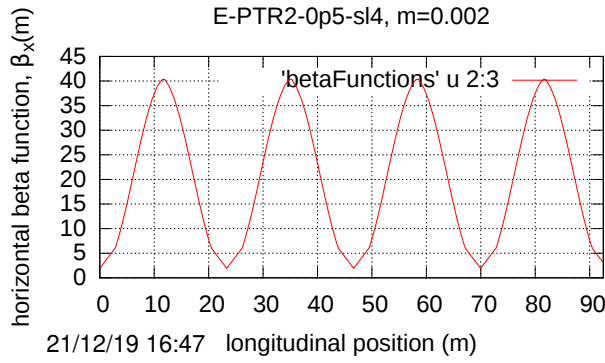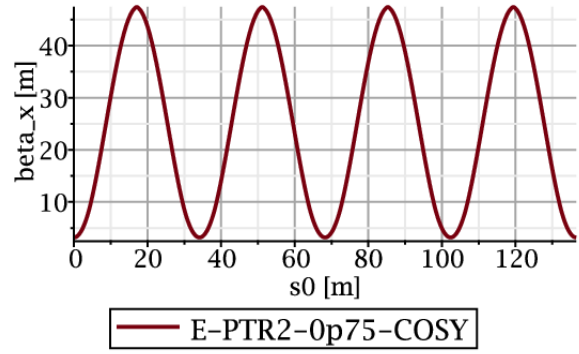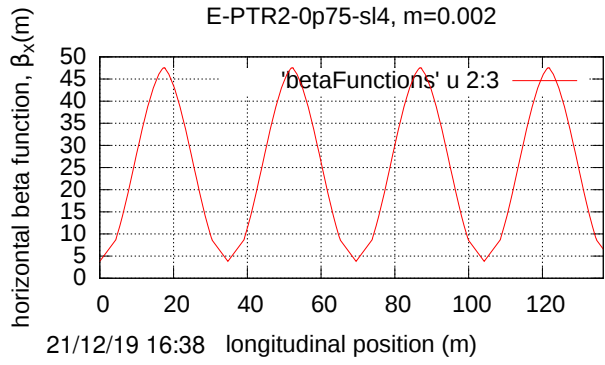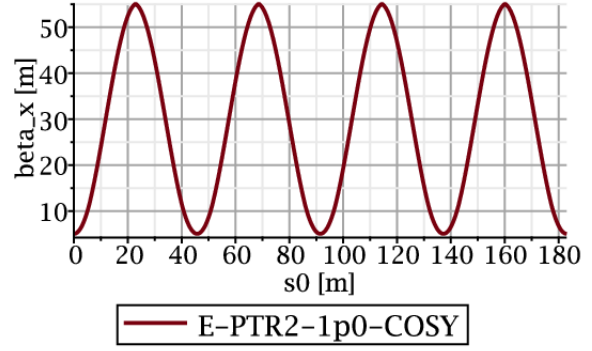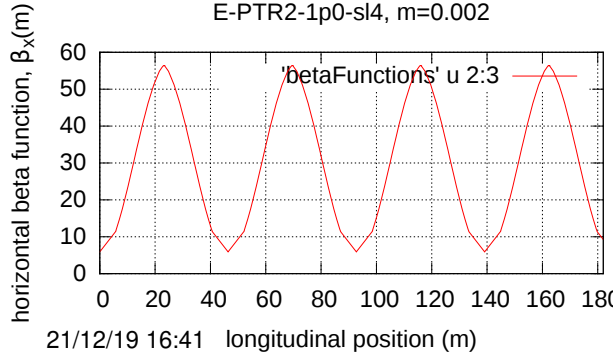
Figure 3: $\beta_x(s)$ calculated by ETEAPOT for the E-PTR2 rings.

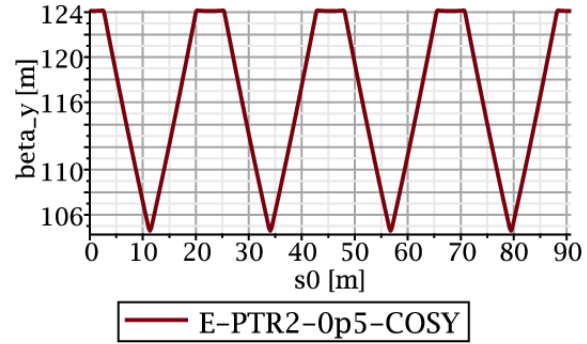Figure 4: $\beta_x(s)$ calculated by MAPLE linearized theory for the E-PTR2 rings.
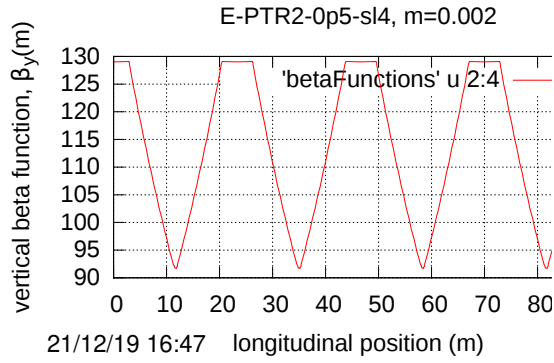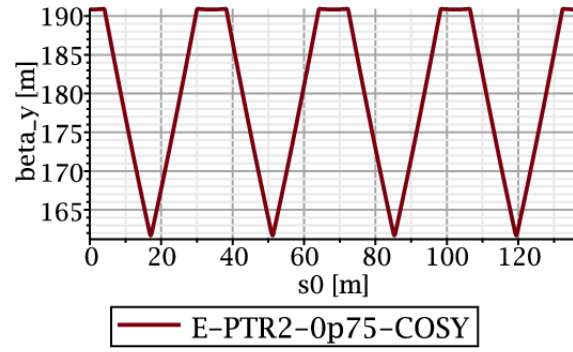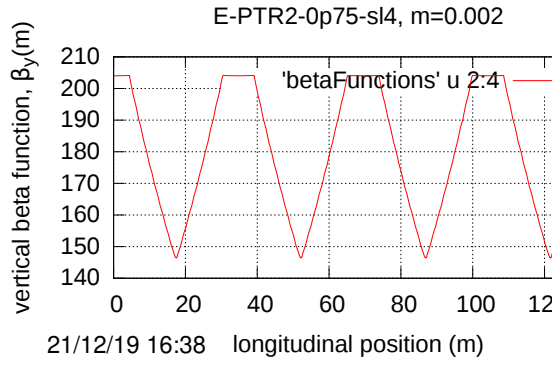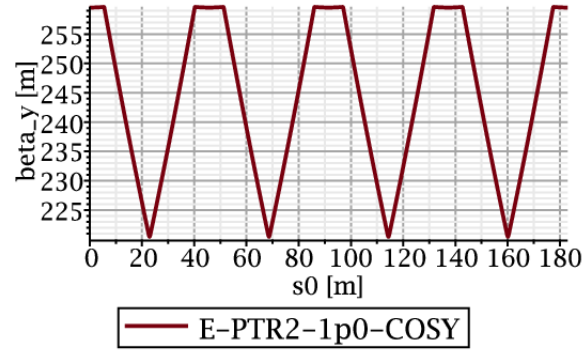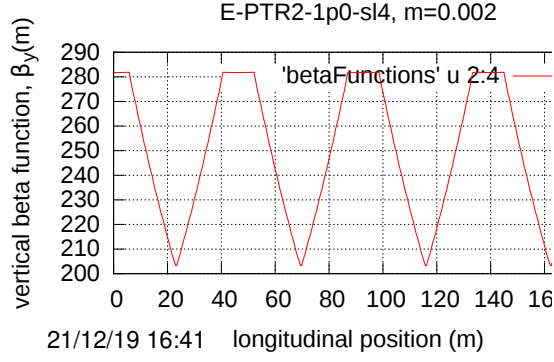
Figure 5: $\beta_y(s)$ calculated by ETEAPOT the E-PTR2 rings.

Figure 6: $\beta_y(s)$ calculated by MAPLE linearized theory for the E-PTR2 rings.
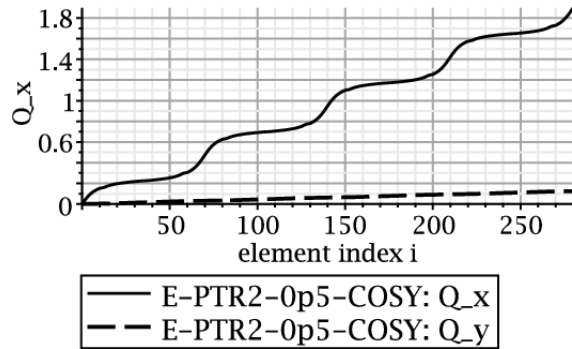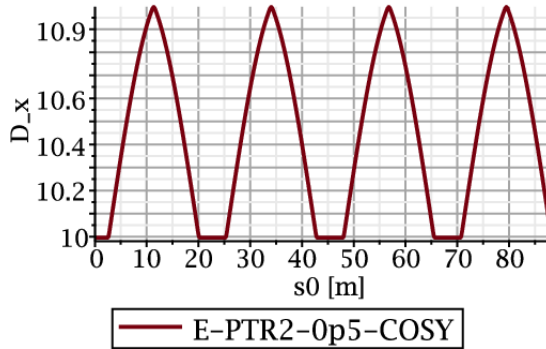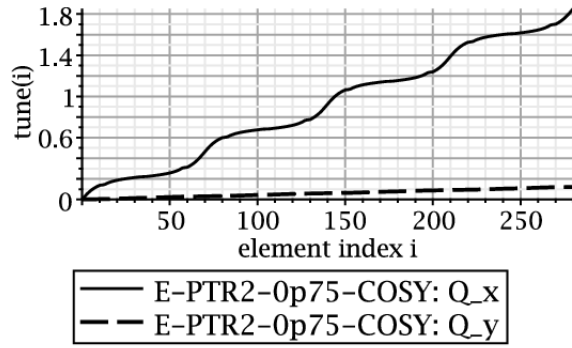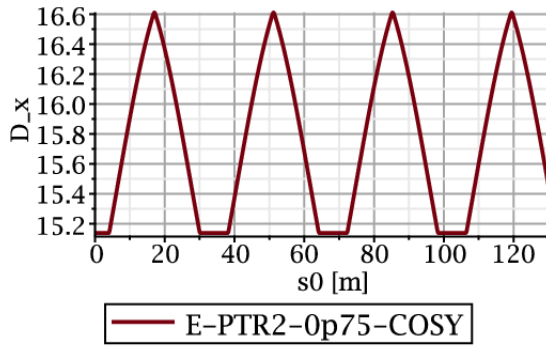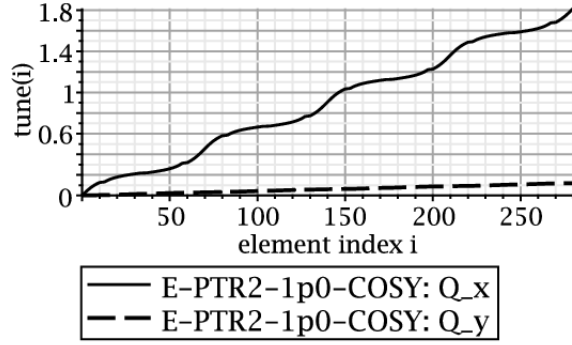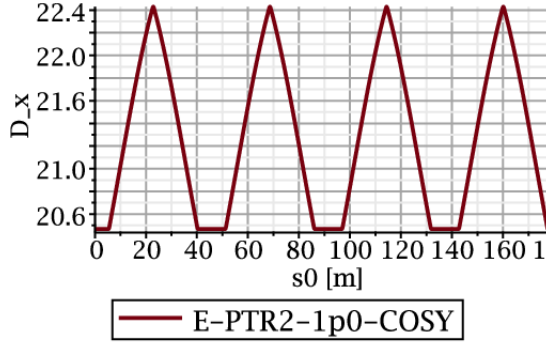
Figure 7: $D(s)$ calculated by MAPLE linearized theory for the `E-PTR2` rings.

Figure 8: calculated by MAPLE linearized theory for the `E-PTR2` rings.

10

Table 3: MAPLE/ETEAPOT comparisons for lattice `E-PTR2-0p5-COSY`

parameter	parameter name	unit	ETEAPOT [-0.032]	MAPLE
super-periodicity	N_S		4	4
bend radius	`r0`	m	10.0	10.0
long straight length	`llstot`	m	6.0	6.0
half bend per cell	$\Theta = \pi/N_\mathrm{S}$	r	0.785398	0.785398
half bend length	`leh`	m	3.92699	3.92699
circumference	$\mathcal{C}$	m	90.832	90.832
quad strengths	qF, qD	1/m	0.01, -0.01	0.01, -0.01
(alternating) field index	m		± 0.002	± 0.002
electric field, 30 MeV p	E	MV/m	5.91	5.91
electrode voltages	V	KV	± 206.7	± 206.7
electrode separation	gap	cm	7	7
horz beta, min/max	β_x	m	1.919, 40.0	1.04, 39.5
vert beta, min/max	β_y	m	90.2, 129.0	104.6, 124.9
dispersion, max,min	D_x	m		10.00, 10.99
horizontal tune	`Qx`		1.833	1.898
vertical tune	`Qy`		0.1320	0.1247

Table 4: MAPLE/ETEAPOT comparisons for lattice `E-PTR2-0p75-COSY`

parameter	parameter name	unit	ETEAPOT [-0.032]	MAPLE
super-periodicity	N_S		4	4
bend radius	`r0`	m	15.4	15.4
long straight length	`llstot`	m	8.932	8.932
half bend per cell	$\Theta = \pi/N_\mathrm{S}$	r	0.785398	0.785398
half bend length	`leh`	m	6.047	6.047
circumference	$\mathcal{C}$	m	136.49	136.49
quad strengths	qF, qD	1/m	0.0065, -0.0065	0.0065, -0.0065
(alternating) field index	m		± 0.002	± 0.002
electric field, 30 MeV p	E	MV/m	3.836	3.836
electrode voltages	V	KV	± 134.2	± 134.2
electrode separation	gap	cm	7	7
horz beta, min/max	β_x	m	3.809, 46.5	3.183, 47.43
vert beta, min/max	β_y	m	149, 204.0	161.7, 190.8
dispersion, max,min	D_x	m		15.2, 16.6
horizontal tune	`Qx`		1.776	1.851
vertical tune	`Qy`		0.1237	0.1214

Table 5: MAPLE/ETEAPOT comparisons for lattice `E-PTR2-1p0-COSY`

parameter	parameter name	unit	ETEAPOT [-0.032]	MAPLE
super-periodicity	N_S		4	4
bend radius	`r0`	m	21.0	21.0
long straight length	`llstot`	m	11.760	11.760
half bend per cell	$\Theta = \pi/N_\mathrm{S}$	r	0.785398	0.785398
half bend length	`leh`	m	8.247	8.247
circumference	$\mathcal{C}$	m	183.0	183.0
quad strengths	qF, qD	1/m	0.00476, -0.00476	0.00476, -0.00476
(alternating) field index	m		± 0.002	± 0.002
electric field, 30 MeV p	E	MV/m	2.813	2.813
electrode voltages	V	KV	± 98.45	± 98.45
electrode separation	gap	cm	7	7
horz beta, min/max	β_x	m	5.898, 5.642	5.061, 55.08
vert beta, min/max	β_y	m	203.6, 281.8	220.7, 259.5
dispersion, max,min	D_x	m		20.5, 22.4
horizontal tune	`Qx`		1.7390	1.8163
vertical tune	`Qy`		0.1193	0.1196

References

[1] F. Abusaif, et al., *Storage Ring to Search for Electric Dipole Moments of Charged Particles: Feasibility Study,* ArXiv: 1912.07881v2 [hep-ex], 2019

[2] V. Lebedev, *Limitations on an EDM Ring Desin,* EDM collaboration meetings, Forschenszentrum Juelich, November 10-11, 2014, and March 13, 2015

[3] R. Talman and J. Talman, *Electric dipole moment planning with a resurrected BNL Alternating Gradient Synchrotron electron analog ring,* PRST-AB, 18, 074004, 2015

[4] R. Talman and J. Talman, *ETEAPOT: symplectic orbit/spin tracking code for all-electric storage rings,* PRST-AB, 18, 074003, 2015

[5] L. Schachinger and R. Talman, *TEAPOT: A Thin-element accelerator program for optics and tracking,* Particle Accelerators, **22**, p35, 1987

[6] R. Hinkins, L. Schachinger, and R.Talman, *Synchrotron Oscillations in the SSC with TEAPOT,* Proceedings of 1986 Snowmass Meeting. SSC-N-217, July, 1986

[7] A. Chao et al., *Optimization of the Cell Lattice Parameters for the SSC,* SSC-SR-1024, October 15, 1986

[8] R. Talman, *Frequency domain storage ring method for electric dipole moment measurement,* arXiv:1508.04366-[physics.acc-ph], 2015

[9] R. Talman, *The Electric Dipole Moment Challenge,* IOP Publishing, 2017

[10] R. Talman, *A doubly-magic storage ring EDM measurement method,* arXiv:1812.05419-[physics.acc-ph], 2018

[11] R. Talman, *Prospects for Electric Dipole Moment Measurement Using Electrostati Accelerators,* in RIST Volume 10, *The Future of Acxcelerators,* A. Chao and W. Chou editors, 2019

A   Lattice description files

A.1   E-PTR2-0p75-COSY-con-sl4.xml

```
<xsl:transform version="1.0" xmlns:xsl="http://www.w3.org/1999/XSL/Transform"
   xmlns:xsi="http://www.w3.org/2001/XMLSchema-instance" xmlns:saxon="http://icl.com/saxon"
   xmlns:math="http://exslt.org/math" extension-element-prefixes="saxon math">
   <xsl:variable name="pi" select="3.14159265359"/>
   <xsl:variable name="twopi" select="2*$pi"/>
   <xsl:variable name="tiny" select="0.0000000001"/>
   <xsl:variable name="mcsq" select="0.93827231"/>
   <xsl:variable name="G" select="1.7928474"/>
   <xsl:variable name="c" select="299792458.0"/>
   <xsl:variable name="g" select="2*$G + 2"/>
   <xsl:variable name="R_NOMINAL" select="15.4"/>
   <xsl:variable name="L_LONG_STRAIGHT" select="0.58*$R_NOMINAL"/>
   <xsl:variable name="N_SUPER" select="4"/>
   <xsl:variable name="M_NOMINAL" select="0.002"/>
   <xsl:variable name="TWEAK_LENGTHS" select="1.0"/>
   <xsl:variable name="K0" select="0.030"/>
   <xsl:variable name="Escr0" select="$mcsq + $K0"/>
   <xsl:variable name="gamma0" select="$Escr0 div $mcsq"/>
```

```
    <xsl:variable name="p0c" select="math:sqrt($Escr0*$Escr0 - $mcsq*$mcsq)"/>
    <xsl:variable name="beta0" select="$p0c div $Escr0"/>
    <xsl:variable name="m_in" select="4*$M_NOMINAL div $N_SUPER"/>
    <xsl:variable name="Nsl" select="4"/>
    <xsl:variable name="thetah" select="$pi div $N_SUPER div 2"/>
    <xsl:variable name="thetahsl" select="$pi div $N_SUPER div 2 div $Nsl"/>

    <xsl:variable name="etaE" select="1.0"/>
    <xsl:variable name="etaM" select="(1.0-$etaE)"/>
    <xsl:variable name="r0" select="$R_NOMINAL*$TWEAK_LENGTHS"/>
    <xsl:variable name="leh" select="$thetah*$r0"/>
    <xsl:variable name="lehsl" select="$thetah*$r0 div $Nsl"/>

    <xsl:variable name="lss" select="0.8*$TWEAK_LENGTHS"/>
    <xsl:variable name="lssh" select="$lss div 2"/>
    <xsl:variable name="lssq" select="$lss div 4"/>
    <xsl:variable name="llstot" select="$L_LONG_STRAIGHT*$TWEAK_LENGTHS"/>
    <xsl:variable name="llsh" select="($llstot - $lss) div 2"/>
    <xsl:variable name="llshsl" select="($llstot - $lss) div 2 div 4"/>
    <xsl:variable name="lq" select="$lss div 4"/>
    <xsl:variable name="lqh" select="$lq div 2"/>
    <xsl:variable name="qFh" select="-0.01 div $TWEAK_LENGTHS * 10.0 div $R_NOMINAL"/>
    <xsl:variable name="qDh" select=" 0.01 div $TWEAK_LENGTHS * 10.0 div $R_NOMINAL"/>
    <xsl:variable name="totalstraight" select="$N_SUPER*($llstot + $lss)"/>
    <xsl:variable name="circumference" select="2*$pi*$r0 + $totalstraight"/>
    <xsl:variable name="gBy2" select="0.035"/>
    <xsl:variable name="rfvolt" select="0.000001"/>
    <xsl:variable name="rfharmon" select="1"/>
    <xsl:variable name="rflag" select="0.5"/>
    <xsl:variable name="Trev0" select="$circumference div $beta0 div $c"/>
</xsl:transform>
```

A.2 E-PTR2-0p75-COSY-nocon-sl4.xml

```
<xsl:transform version="1.0" xmlns:xsl="http://www.w3.org/1999/XSL/Transform"
    xmlns:xsi="http://www.w3.org/2001/XMLSchema-instance" xmlns:saxon="http://icl.com/saxon"
    xmlns:math="http://exslt.org/math" extension-element-prefixes="saxon math">
    <xsi:elements>
        <element name="mbegin" type="marker"/>
        <element name="mend" type="marker"/>
        <element name="mPeriod" type="marker"/>
        <element name="mhalf" type="marker"/>
        <element name="mQD" type="marker"/>
        <element name="mQF" type="marker"/>

        <element name="RF1" type="rfcavity" l="$tiny">
            <mfield volt="$rfvolt" harmon="$rfharmon" lag='$rflag'/>
        </element>

        <element name="Dlshsl" type="drift" l="$llshsl"/>
        <element name="Dssq" type="drift" l="$lssq"/>

        <element name="QFh" type="quadrupole" l="$lqh">
```

```xml
            <mfield a="0" b="$qFh"/>
        </element>

        <element name="QDh" type="quadrupole" l="$lq">
            <mfield a="0" b="$qDh"/>
        </element>

        <element name="BhMisl" type="sbend" l="$lehsl">
            <mfield a="0" b="concat($etaE*$thetahsl,' ',$m_in*$etaE*$thetahsl)"/>
        </element>

        <element name="BhPlsl" type="sbend" l="$lehsl">
            <mfield a="0" b="concat($etaE*$thetahsl,' ',-$m_in*$etaE*$thetahsl)"/>
        </element>

</xsi:elements>
<!--  -->
<xsi:sectors>

    <sector name="lsin">
        <frame ref="Dlshsl"/>
        <frame ref="Dlshsl"/>
        <frame ref="Dlshsl"/>
        <frame ref="Dlshsl"/>
        <frame ref="Dssq"/>
        <frame ref="mQF"/>
        <frame ref="QFh"/>
        <frame ref="mQF"/>
        <frame ref="mQF"/>
        <frame ref="QFh"/>
        <frame ref="mQF"/>
        <frame ref="Dssq"/>
    </sector>

    <sector name="PM">
        <frame ref="BhPlsl"/>
        <frame ref="BhPlsl"/>
        <frame ref="BhPlsl"/>
        <frame ref="BhPlsl"/>
        <frame ref="BhMisl"/>
        <frame ref="BhMisl"/>
        <frame ref="BhMisl"/>
        <frame ref="BhMisl"/>
    </sector>

    <sector name="QDQD">
        <frame ref="Dssq"/>
        <frame ref="mQD"/>
        <frame ref="QDh"/>
        <frame ref="mQD"/>
        <frame ref="QDh"/>
        <frame ref="mQD"/>
        <frame ref="mQD"/>
```

```xml
        <frame ref="QDh"/>
        <frame ref="mQD"/>
        <frame ref="QDh"/>
        <frame ref="mQD"/>
        <frame ref="Dssq"/>
    </sector>

    <sector name="MP">
        <frame ref="BhMisl"/>
        <frame ref="BhMisl"/>
        <frame ref="BhMisl"/>
        <frame ref="BhMisl"/>
        <frame ref="BhPlsl"/>
        <frame ref="BhPlsl"/>
        <frame ref="BhPlsl"/>
        <frame ref="BhPlsl"/>
    </sector>

<sector name="lsout">
        <frame ref="Dssq"/>
        <frame ref="mQF"/>
        <frame ref="QFh"/>
        <frame ref="mQF"/>
        <frame ref="mQF"/>
        <frame ref="QFh"/>
        <frame ref="mQF"/>
        <frame ref="Dssq"/>
        <frame ref="Dlshsl"/>
        <frame ref="Dlshsl"/>
        <frame ref="Dlshsl"/>
        <frame ref="Dlshsl"/>
    </sector>

    <sector name="period">
        <frame ref="lsin"/>
        <frame ref="PM"/>
        <frame ref="QDQD"/>
        <frame ref="MP"/>
        <frame ref="lsout"/>
    </sector>

    <sector name="ring">
        <frame ref="mbegin"/>
        <frame ref="mPeriod"/>
        <frame ref="period"/>
        <frame ref="mPeriod"/>
        <frame ref="period"/>
        <frame ref="mPeriod"/>
        <frame ref="mhalf"/>
        <frame ref="mPeriod"/>
        <frame ref="period"/>
        <frame ref="mPeriod"/>
        <frame ref="period"/>
```

```
                <frame ref="mPeriod"/>
                <frame ref="mend"/>
            </sector>
        </xsi:sectors>
</xsl:transform>
```